Journal of Applied Electrochemistry (2024) 54:163–174
https://doi.org/10.1007/s10800-023-01937-5

RESEARCH ARTICLE

Mobile-assisted diagnostic biosensor for point-of-care glucose detection in real human samples with rapid response and long-live stability

Artur Jędrzak[1] · Maria Kuznowicz[1] · Teofil Jesionowski[1]

Received: 17 March 2023 / Accepted: 11 June 2023 / Published online: 26 June 2023

Abstract

In this work, the β-cyclodextrins (βCD) grafted on magnetite@polynorepinephrine (Fe_3O_4@PNE) nanomaterial with glucose oxidase (GOx) from *Aspergillus niger* was presented. The electroactive nanoplatform was used to construct rapid response and long-live time biosensor for qualitative and quantitative glucose determination. The nanomaterial was deposited on the screen-printed electrode (SPE) and integrated with the potentiostat in tandem with a portable devices. The methodology may affect its relatively low unit cost, miniaturization aspect, and electrode system integrity. The potential usage is intended for advanced diabetes care with a focus on the point-of-care testing idea. The cyclic voltammetry and amperometry were used for electrochemical characterization. The presented SPE/Fe_3O_4@PNE@βCD-GOx biosensor enabled measurements in a wide range of concentrations (0.1–30.0 mM), an enhanced sensitivity (204.82 μA mM^{-1} cm^{-2}), a low limit of detection (3.2 μM), and a rapid response (2.6 s). Moreover, the proposed sensor achieved long-term stability, up to 11 months. Testing on real samples (human blood, human serum, infusion fluids) showed recovery in range from 95.5 to 98.6%. The outcomes demonstrated that this biosensor has great potential for use in determining the amount of glucose in a biological fluids and commercial products. The novelty of this work would largely consist of the possibility of qualitative and quantitative measurements of glucose in real human samples with a long time stability. This portable system enables mobile diagnostics tests including point-of-care testing idea. Due to the applied β-cyclodextrins on the surface of the novel polynorepinephrine biopolymer coating, selectivity, stability, and sensitivity were improved.

Graphical Abstract

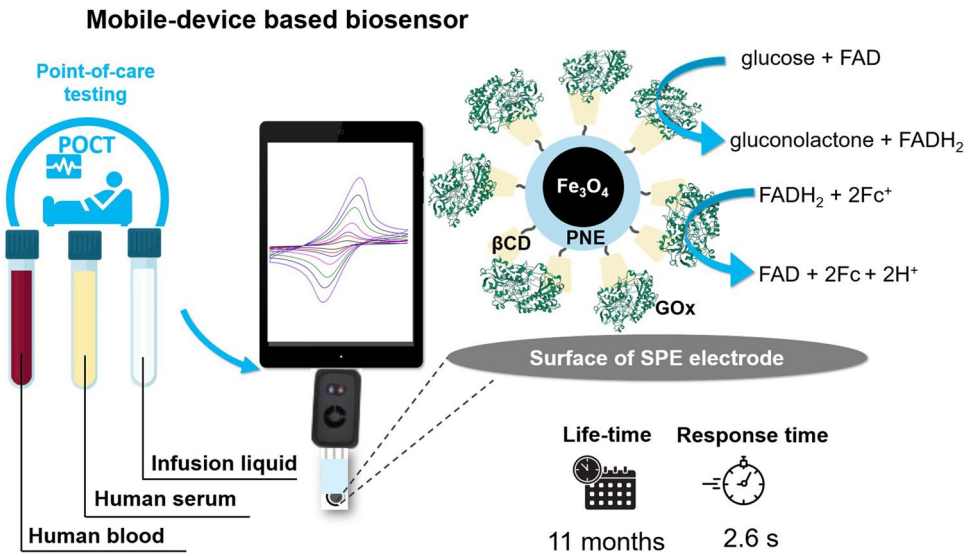

Extended author information available on the last page of the article

Keywords Analytical determination of glucose · Electrochemical biosensor · Point-of-care testing · Polynorepinephrine

1 Introduction

The development of effective diagnostic tools for precise, simple, and rapid glucose detection in body fluids is a key factor in the advancement of medicine [1]. Currently, the common part of diabetes mellitus treatment relies on self-monitoring using glucometers [1]. However, there are still scientific reports about numerous errors in the devices resulting from manufacturing techniques, premature aging, impropriate storage, or incorrect use [2].

Nowadays, one of the most accurate glucose detection techniques is still in hospital trials, mainly photometric chemical analyzers [3]. Following the several advantages of these devices like high sensitivity, precision, and selectivity, they contain limitations resulting from the unit cost of the apparatus, service, maintenance, and staff training [4, 5]. Common curses for the patients are still the need to come to specialist units, i.e. hospitals or diagnostic institutions, queues, turnaround time, transport samples to an analytical laboratory, and re-consultation with the medical crew [6]. Moreover, in recent years, non-enzymatic systems for glucose detection and other analytes, enabling measurements without the use of enzymes, have become an alternative in the sensor market [7-9]. Resulting from properly designed, obtained, and characterized nanomaterials that allow for use in (bio)sensor systems [10-12].

A new way for glucose measurements is a mobile-based point-of-care testing (POCT) idea as a part of telemedicine [3]. POCT is an alternative method to central or core laboratory testing. In this technique, diagnostic procedures are carried out close to the location of the patient [6]. In addition, the method enables easy detection, without the need to involve the laboratory staff and without the patient's movement [13]. The trend of POCT due to easy data sharing is an alternative to traditional and complex test methods, which significantly extended the time of the analysis itself and finally delayed the possibility of treating patients [14]. Moreover, POCT is part of advanced diabetes care, which provides advanced and individual health care plans.

The higher development of mobile POCT sensor technology was caused by the pandemia of COVID-19, which spread at the turn of the years 2019/2020, and continues to this day. As a result, POCT devices with easy data transfer grew in popularity and turned out to be a very necessary tool for caring the patient's health. Through this expansion, the idea of research without leaving home has gained popularity and hence more interest in mobile-based biosensors [15].

Polydopamine (PDA) coatings were presented by Lee et al. in 2007, motivated by the adhesion behavior of mussels [16]. The adhesive properties of this biopolymer were widely used in the immobilization of biomolecules and later in the construction of biosensors. Using PDA enabled effective and time-stable attachment of enzymes [17]. However, despite the coating ability of PDA, uncontrolled roughness during PDA polymerization limits the wide application of PDA, and has forced the search for new biomimetic polymers. Due to the significant difference between catecholamine coatings derived from different monomers, another novel approach may be the use of polynorepinephrine (PNE). It was proven that the PNE coating is much smoother than PDA, which can significantly affect the application, including the attachment of biomolecules and the final properties of the sensors [17, 18].

In this work, we present the biosensor that may be an attractive alternative for rapid, portable, and long-term stability of glucose measurement with the possibility of easy data sharing. Detection of glucose in real samples such as human serum, human blood, and infusion fluids were carried out. This biosensor complies with the latest FDA guidelines related to the construction of new glucometers [19]. The multicomponent system proposed in the work is characterized by unique properties. Magnetite is characterized by magnetic abilities which enable easy separation and may significantly increase the thermal stability of the material. Polynorepinephrine is a quite new biomimetic polymer that easily functionalizes surfaces with strong adhesive properties and allows protect the magnetic core. β-cyclodextrins play a crucial role as nanocontainers greatly affect the effectiveness of the immobilization process and improved the time stability of the sensor system [5].

In addition, it was hypothesized that the created multicomponent material would improve the properties of the biosensor, i.e. sensitivity, linearity range, and in particular, it would improve the stability of the biosensor over time due to the β-cyclodextrins applied. The novelty of the research would largely consist of the possibility of sensitive, selective measurements for a long time of using the biosensor, and working in tandem with a mobile device. This whole system enables the mobility of measurements (mobile analytes monitoring stations), resulting in availability, ease of use, and reduced unit costs due to the low-cost components.

It is also significant that when this work was undertaken, there were no existing literature reports on this type of tandem system (potentiostat—mobile devices) with the magnetite@polynorepinephrine@β-cyclodextrins-glucose oxidase nanomaterials for glucose detection.

2 Materials and methods

2.1 Chemicals and materials

Substrates for obtaining a hybrid material such as iron(II) chloride tetrahydrate ($FeCl_2{\cdot}4H_2O$), iron(III) chloride hexahydrate ($FeCl_3{\cdot}6H_2O$), ammonia solution (25%), norepinephrine hydrochloride (NE·HCl), β-cyclodextrins (βCD), phosphate buffer saline (PBS), citric buffer, glucose oxidase from *Aspergillus niger* (protein content 65–85%, molecular weight 160 kDa), tris(hydroxymethyl)aminomethane (TRIS) were provided from Merck, Germany. Reagents for electrochemical tests: α-D-glucose, (hydroxymethyl)ferrocene (HFc), human serum, fructose, maltose, sucrose, uric acid, ascorbic acid, L-cysteine, and dopamine were purchased from Merck, Germany. Bio-Rad (USA) provided samples of human blood. Screen-printed electrodes (SPE) were purchased from Metrohm DropSens. Working electrode (4 mm diameter) and counter electrodes was made of carbon. The reference electrode was made of silver. All of the chemicals were of analytical-grade quality.

2.2 Synthesis of Fe_3O_4@PNE@βCD hybrid nanomaterial

The co-precipitation method was used to obtain magnetite nanoparticles. In 100 mL Milli-Q® water, $FeCl_3{\cdot}6H_2O$ (3.44 g; 11.09 mM) and $FeCl_2{\cdot}4H_2O$ (1.72 g; 7.55 mM) were dissolved and heated to 90 °C. The synthesis was carried out under a nitrogen gas environment, which reduced the amount of oxygen in the solution, and 20 mL of 25% aqueous ammonia was supplied dropwise. After 30 min, the system was cooled to ambient temperature. The reaction for obtaining magnetite by the co-precipitation method is shown in Fig. 1A.

To coat the nanoparticles with polynorepinephrine 200 mL TRIS buffer solution (pH 8.5, 10 mM) was added to 100 mg magnetite nanoparticles. After sonicating the solution to homogeneity, 100 mg of norepinephrine was added (0.87 mM). The process was carried out for 24 h with continuous mixing conditions (Fig. 1B). The material was then washed several times with distilled water to remove unreacted substrates.

Further, the β-cyclodextrins were linked to the Fe_3O_4@PNE material via thiol-Michael reaction. To obtain the Fe_3O_4@PNE@βCD nanoplatform, 100 mg of Fe_3O_4@PNE material was added to 200 mL of TRIS buffer solution (pH 8.5; 10 mM). Next, 200 mg of 6-monodeoxy-6-monothio-β-cyclodextrins (SH-βCD) was added to the carrier. At ambient temperature, the synthesis was continued for another 24 h. After the synthesis, the material was cleaned by washing several times. Reaction schemes are presented in Fig. 1C.

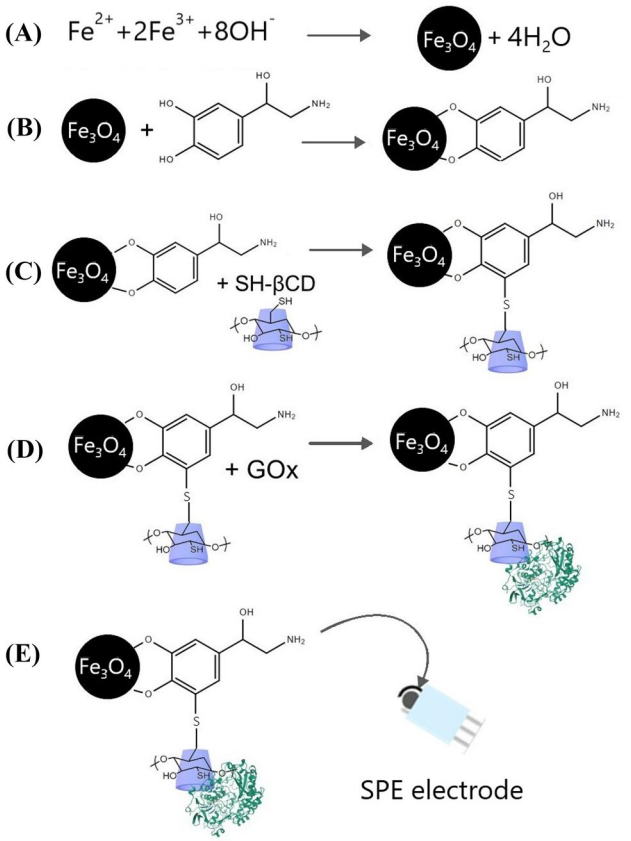

Fig. 1 Schematic representation of magnetite nanoparticles obtained by co-precipitation method (**A**); polymerization of NE · HCl on the Fe_3O_4 nanoparticles (**B**); SH-βCD addition to Fe_3O_4@PNE via thiol-Michael reaction (**C**); glucose oxidase immobilization on the nanomaterial (**D**); SPE electrode modification with the Fe_3O_4@PNE @βCD-GOx (**E**)

2.3 Immobilization of GOx on the nanoplatforms

To immobilize the enzyme using the adsorption technique, 5 mg of nanomaterial (Fe_3O_4, Fe_3O_4@PNE, or Fe_3O_4@PNE@βCD) and 0.5 mg of glucose oxidase were added. The immobilizations at varied time intervals (1, 2, 8, 12, 24, and 48 h) were done. The process of immobilization is presented schematically in Fig. 1D.

2.4 Fabrication of SPE/Fe_3O_4@PNE-GOx and SPE/Fe_3O_4@PNE@βCD-GOx electrodes

The resultant Fe_3O_4@PNE-GOx (5.32 mg mL^{-1}) and Fe_3O_4@PNE@βCD-GOx.

(6.75 mg mL^{-1}) nanomaterials were dropped on the surface of a screen-printed electrode (SPE) and allowed to dry

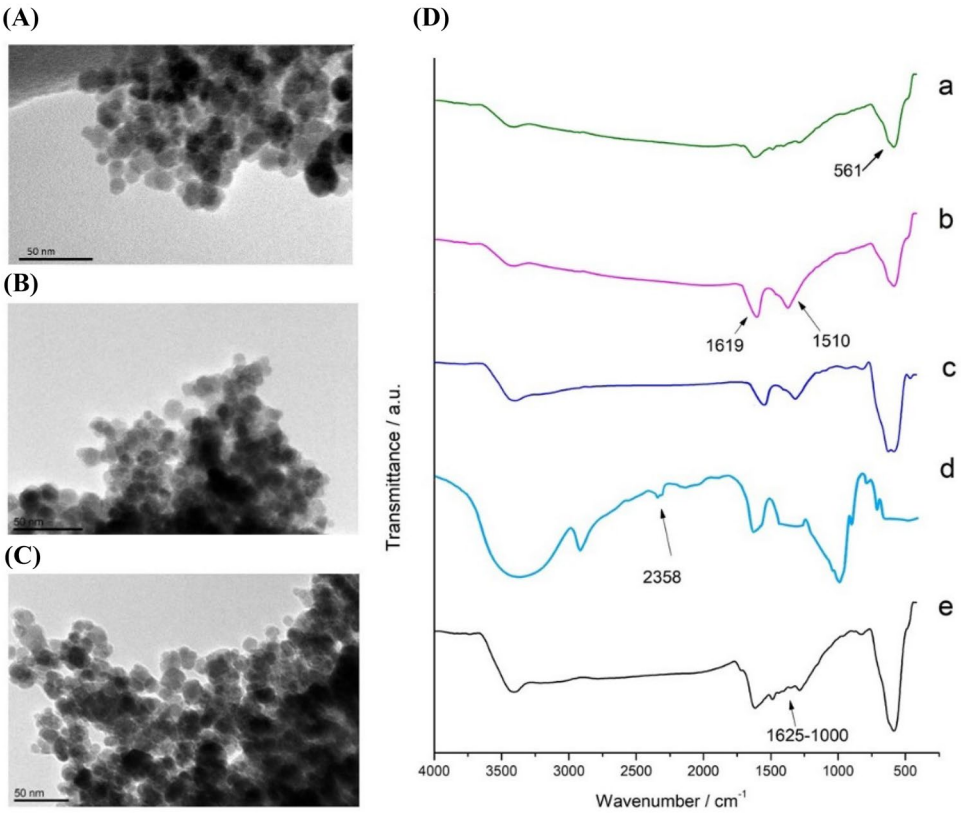

Fig. 2 Transmission electron microscopy (TEM) micrographs of the synthesized bare Fe_3O_4 (**A**); Fe_3O_4@PNE nanomaterial (**B**); Fe_3O_4@PNE@βCD nanoplatform (**C**); FT-IR spectra (**D**) of: Fe_3O_4 (a); Fe_3O_4@PNE (b); Fe_3O_4@PNE@βCD (c); SH-βCD (d); and Fe_3O_4@PNE@βCD-GOx (e)

at ambient temperature. This step is schematically shown in Fig. 1E.

2.5 Physicochemical analysis

A Jeol analyzer (JEM-1400) with a resolution of 2 nm and a maximum acceleration of 120 kV was used to conduct the transmission electron microscopy (TEM) investigation. Fourier transform infrared spectroscopy (FTIR) was used to determine the functional groups contained in the hybrid platforms' structure. A Vertex 70 spectrometer was used to obtain the FTIR spectra. The nanomaterials were tested as tablets, which were formed by mixing 2 mg of the test ingredient with 250 mg of anhydrous KBr at a 10 MPa pressure. In air conditions, atomic force microscopy (AFM) was performed with an Agilent 5500 in intermittent contact mode. Polydispersity index (PDI) values were measured using a Zetasizer Nano ZS with a range of 0.6–6000 nm to test the materials' stability in a liquid solvent. The same apparatus was used to determine the zeta potential (ζ) and to obtain zeta potential values.

2.6 Electrochemical study

The electrochemical tests were carried out with the smallest ready-to-go Sensit Smart potentiostat (Palmsens, the Netherlands), which is compatible with mobile device like smartphones and tablets. All tests with glucose solutions were carried out in PBS (10 mM; pH 7.4) with a 10 mM mediator (hydroxymethyl)ferrocene (HFc). In the case of CV studies, tests were carried out in the range of potentials between −0.2 and 0.6 V at a scan rate of 10 mV s^{-1}. The tests with the use of amperometry were carried out at a potential of 0.3 V.

The stability over time was tested for 11 months on the same electrode, which was stored at 4 °C. Human blood, human serum, and infusion fluids were carried out as real samples of glucose. This research was examined using the standard addition method. Moreover, the obtained results were compared with 3 commercial blood glucometers.

3 Results and discussion

3.1 Morphological characterization

The prepared Fe_3O_4 NPs, Fe_3O_4@PNE, and Fe_3O_4@PNE@βCD nanomaterials were characterized by transmission electron microscopy (TEM). Figure 2 A presented the magnetite nanoparticles with diameter sizes in the range of 7–12 nm. These nanoparticles were characterized by a uniformly spherical shape. In Fig. 2B the core–shell structured Fe_3O_4@PNE hybrid nanomaterial was presented. The polynorepinephrine layer was uniformly coated on the

surface of the Fe_3O_4, with thickness distributed in the range of 2–4 nm, which can be observed in the TEM image. In Fig. 2C the structure with β-cyclodextrins is presented. TEM images cannot confirm the attachment of the βCD because of the observed similar structures. To confirm the obtained nanomaterials, further research was carried out, pointing the linked βCD to the magnetite@polynorepinephrine nanoplatform.

To check the effectiveness of obtaining individual materials and the characteristics of functional groups present Fourier transform infrared spectroscopy (FT-IR) was performed. In Fig. 2D, a curve corresponds to bare magnetite nanoparticles. The intense peak observed at 580 cm^{-1} is attributed to the stretching vibration mode associated with the metal–oxygen Fe–O bonds in the Fe_3O_4 NPs. The characteristic FTIR data peaks for Fe_3O_4@PNE (curve b) at the wavenumber with the maximum at 3400 cm^{-1} corresponding to the –OH group [20]. There are also characteristic bands corresponding at 1510 and 1619 cm^{-1} corresponding to phenol [20]. Curve c shows the material after β-cyclodextrins attachment. Moreover, the disappearance of the –SH absorption peak 2358 cm^{-1} indicates that βCD was successfully attached to the surface of Fe_3O_4@PNE hybrid nanomaterial [21]. The effectiveness of the adsorption immobilization of the enzyme on the matrix surface was confirmed by signals at the wave number in the range of 1600−1000 cm^{-1}. Corresponding to 1625 cm^{-1} groups: amide I; 1525 cm^{-1}: amide II; 1030 cm^{-1}: C–O and additional signals with a wave number of around 3950 cm^{-1} (N–H) [22].

3.2 Evaluation of particle size and uniformity of dispersion

The stability and effectiveness of the individual materials Fe_3O_4, Fe_3O_4@PNE, and Fe_3O_4@PNE@βCD were checked using electrokinetic analysis at a constant pH of 7.0 (Table S1, see Supplementary Material). The highest value of the zeta potential was measured for magnetite nanoparticles and was − 41.3 mV. Indicating the high stability of the Fe_3O_4 colloid in the measured solution of electrolyte. Individual modifications of these nanoparticles caused the zeta potential value to drop to − 23.8 and − 20.5 mV for Fe_3O_4@PNE and Fe_3O_4@PNE@βCD, respectively. This suggests that conducted modifications may reduce the electrostatic repulsion between the nanoparticles and indicate the components being attached. All obtained zeta potential values may be still classified as an electrokinetically stable material.

The polydispersity index (PdI) value for Fe_3O_4 obtained from the NIBS analysis showed an increase in particle size which is summarized in Table S1 (see Supplementary Material). A low PdI (0.186) for magnetite nanoparticles indicates that they are stable in colloidal form. The polydispersity index for Fe_3O_4@PNE and Fe_3O_4@PNE@βCD was 0.433 and 0.511, respectively, suggesting the polydispersive characteristics of the obtained nanoparticles.

3.3 Immobilization of glucose oxidase (GOx)

Optimization of the glucose oxidase immobilization process was carried out with the use of different nanoplatforms (Fe_3O_4, Fe_3O_4@PNE, Fe_3O_4@PNE@βCD) at different times (1, 2, 4, 8, 12, 24, 48 h). The effectiveness of immobilization was determined via the Bradford method. The obtained results are presented in Fig. 3A.

The highest efficiency of the immobilization process was observed after 24 h for the Fe_3O_4, Fe_3O_4@PNE, and Fe_3O_4@PNE@βCD nanomaterials with the results 16.4, 37.8, and 49.1 mg g^{-1}, respectively (Table S2, see Supplementary Material). The prolonged time may cause the enzyme to leach from the carrier surface.

Moreover, the effectiveness of immobilization on the nanoplatform was compared with other materials used for the immobilization of glucose oxidase presented in the literature in Table 1.

The surface structure of the Fe_3O_4@PNE@βCD material before and after the glucose oxidase (GOx) immobilization process were presented using atomic force microscopy (AFM) (Fig. 3B, C). Significant changes in the material after immobilization were observed, a nearly fourfold increase of the Z parameter, which may suggest the successful GOx attachment. Moreover, before immobilization, the AFM image of the surface can show a relatively smooth and featureless surface. After immobilization, the presence of the immobilized layer can be visualized as a distinct change in the surface morphology. These images provide visual and quantitative (in Z parameter) evidence of successful immobilization and can be used to assess the effectiveness of the immobilization process.

Additionally, height profiles were determined for both nanoplatforms, as shown in Fig. S1 (see Supplementary Material). The roughness coefficient (Sa) of the hybrid material was also evaluated before and after immobilization (Table S3, see also Supplementary Material). The material's Sa value after immobilization is almost two times lower than the matrix's value before GOx adsorption. The reduction of the roughness parameter confirms the smoothing effect of the enzyme on the surface.

3.4 Electrochemical tests of SPE/Fe_3O_4@PNE@βCD-GOx electrode

The Randles–Sevcik equation was used to calculate the electroactive surface area (A) of each electrode, where Ip is the peak current, n is the number of transferred electrons, D is the diffusion coefficient in cm^2 s^{-1}, C is the electroactive

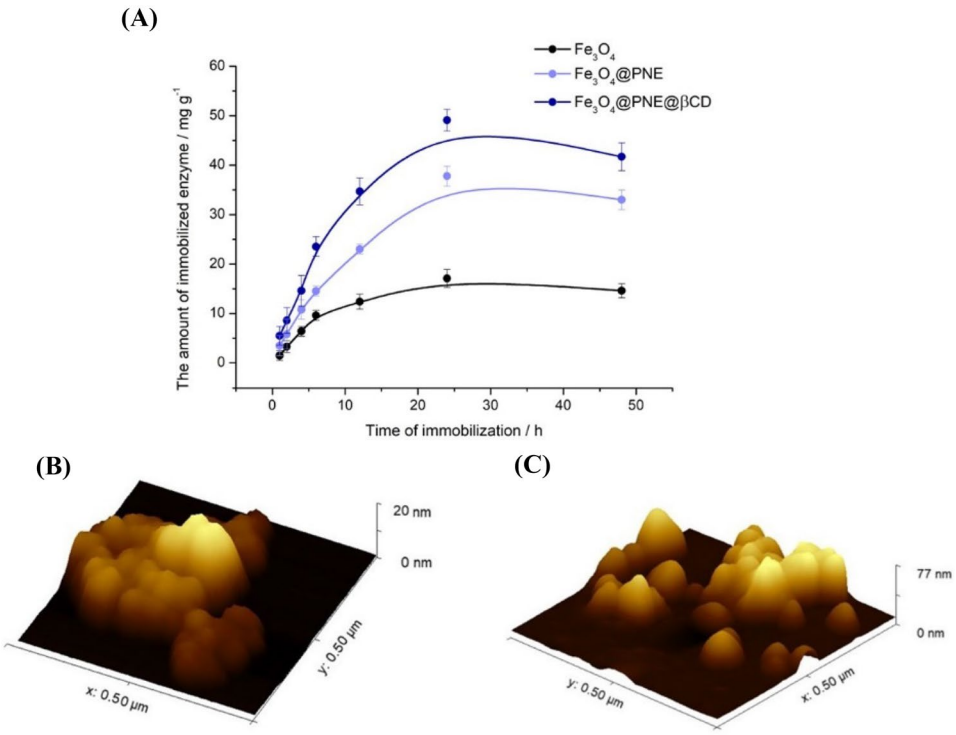

Fig. 3 Quantities of enzyme immobilized on Fe_3O_4, Fe_3O_4@PNE, and Fe_3O_4@PNE@βCD from glucose oxidase solution (5 mg mL^{-1}) at various times ($n = 3$) (**A**); AFM images of Fe_3O_4@PNE@βCD nanomaterial before (**B**); and after GOx immobilization (**C**)

Table 1 Amount of GOx immobilized on various platforms

Immobilization platform	Immobilized GOx / mg g^{-1}	References
Fe_3O_4@PNE	37.8	[5]
Fe_3O_4@PDA@βCD	47.6	[22]
MIMNs	33.0	[23]
Silica	12.9	[24]
Fe_3O_4@PDA	36.3	This work
Fe_3O_4	16.4	This work
Fe_3O_4@PNE@βCD	49.1	This work

species concentration in mol cm^{-3}, and v is the scan rate in V s^{-1} [25].

$$I_p = 2.687 \cdot 10^5 \cdot n^{\frac{3}{2}} \cdot A \cdot D^{\frac{1}{2}} \cdot C \cdot v^{\frac{1}{2}} \quad (1)$$

The electroactive surface area of the paper electrodes was calculated as 0.075 cm^2 for the unmodified SPE electrode, 0.291 cm^2 for the Fe_3O_4@PNE, 0.380 cm^2 for the Fe_3O_4@PNE@βCD and 0.345 cm^2 for the Fe_3O_4@PNE@βCD-GOx electrode presented in Fig. S2 (see Supplementary Material). It was also observed that the higher the active surface of the working electrode, the higher the currents are registered, which is consistent with literature reports [26].

The response of Fe_3O_4@PNE@βCD-GOx modified SPE electrode to changing glucose concentration was investigated by a cyclic voltammogram. The mechanism of glucose oxidation on the surface of the biosensor is presented in Fig. 4A. Figure 4B shows the anodic and cathodic current peaks generated by the addition of glucose concentrations ranging from 1 mM to 180 mM in 50 mM PBS with 10 mM HFc, at a scan rate of 10 mV s^{-1}. The subsequent addition of glucose resulted in a significant increase in current intensity, indicating high electrode sensitivity. In the presence of an external redox mediator—(hydroxymethyl)ferrocene (HFc), the SPE/Fe_3O_4@PNE@βCD-GOx biosensor catalyzes the oxidation of glucose. The reduced form of the HFc is transformed to its catalytically active oxidized form—HFc^+. Then $FADH_2$ and HFc^+ exchange electrons, resulting in the regeneration of FAD and the production of HFc. The electrocatalytic response is proportional to the amount of glucose after HFc acting is reoxidized on the electrode surface.

The dependence between the current value and the glucose concentration presents the characteristic shape of the Michael–Menten kinetics [27] (Fig. 4C), which approaches saturation above 150 mM of glucose. This condition describes the typical behavior of enzymatic reaction phenomena [28].

Moreover, the CV measurements with different scan rates in a range from 5 to 100 mV s^{-1} were also investigated to further verify the bioelectrochemical activity of the SPE/Fe_3O_4@PNE@βCD-GOx electrode. The peak current increased significantly as the scan rate increased, as shown in Fig. S3A (see Supplementary Material). Between 5 and 100 mV s^{-1}, the oxidation and reduction peak currents were directly proportional to the square root of the scan rate (Fig.

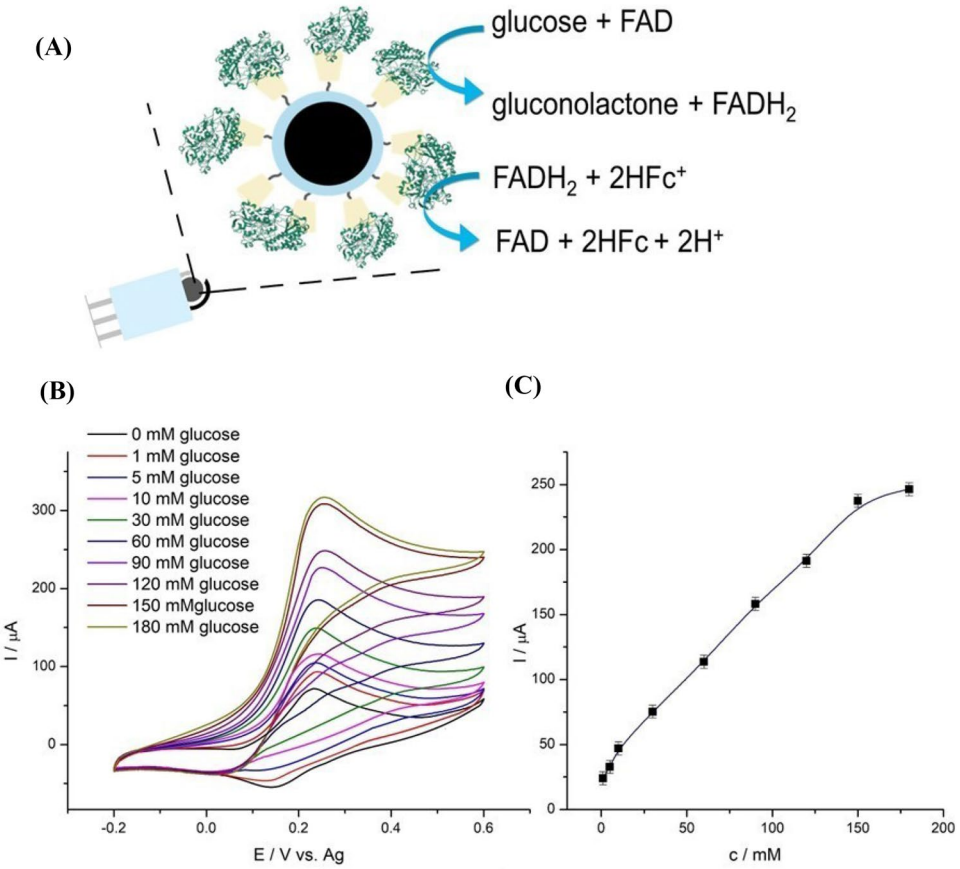

Fig. 4 Schematically presenting the work of the SPE/Fe_3O_4@PNE@βCD-GOx biosensor (**A**); Cyclic voltammograms in PBS solution containing 10 mM HFc and various concentrations of glucose at scan rate 10 mV s^{-1} (**B**); The calibration curve (**C**)

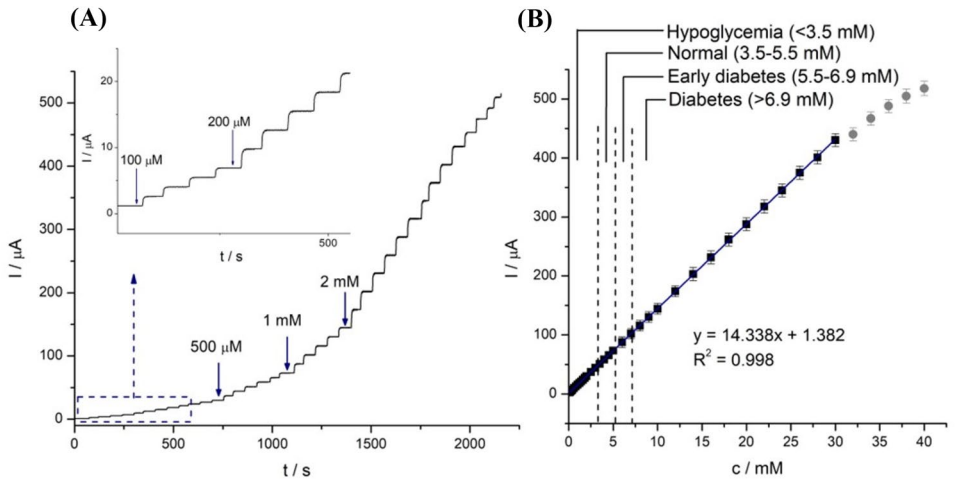

Fig. 5 Amperometric response of SPE/Fe_3O_4@PNE@βCD-GOx biosensor in 10 mM PBS (pH 7.4; 10 mM of HFc) at a working potential of 0.3 V (**A**); The calibration curve with diabetic glucose ranges (**B**)

S3B). The linear correlation R^2 was 0.993 and 0.994, respectively. This suggested that the mass transfer in the modified electrode was regulated by diffusion [28].

Comparative investigations of SPE/Fe_3O_4@PNE@βCD-GOx biosensor were conducted to evaluate the electrochemical response. The biosensor was used to detect glucose with successive additions, as shown in Fig. 5A. The linear relationship between current response and concentration (Fig. 5B) exhibited a good correlation coefficient (R^2) of 0.998 over the concentration range of 0.1–30.0 mM, with a high sensitivity of 204.82 µA $µM^{-1}$ cm^{-2} and a low limit of detection (LOD) of 3.20 µM. The proposed glucose biosensor enables glucose measurement in the whole range of human blood concentrations (hypoglycemia, normal, early diabetes, and diabetes), under the WHO guidelines [29].

The proposed SPE/Fe_3O_4@PNE@βCD-GOx sensor is additionally characterized by a rapid response time of 2.6 s. Compared to the system without βCD, the response is

Table 2 Comparison of the analytical performance of various glucose GOx-based biosensors

Electrode	Sensitivity (μA mM^{-1} cm^{-2})	Limit of detection (μM)	Linear range (mM)	References
GOx-SiO_2/Lig/Fc/CPE	11.0	145.0	0.5–9.0	[23]
GOx/Nafion®/MnO_2-GNR/SPCE	56.32	50.0	0.1–1.4	[30]
Fc-PLL/GOx	6.55	23.0	0–10.0	[31]
GOx/β-CD/MWCNTs/GCE	32.28	0.42	0.05 – 1.15	[32]
LSG/PBSE/PtNPs/GOx/Nafion®	12.64	2.35	0.0025–2.5	[33]
FTO-CNTs/PEI/GOx	63.38	70.0	0.07–0.7	[34]
GODx/Au@C/TiO_2/FTO	29.76	49.0	0.1–1.6	[35]
Au/OPPy/AuNPs/GOx/Nafion®	8.09	40.0	0–2.6	[36]
Fe_3O_4@PNE-GOx	97.30	6.10	0.2–24.0	[5]
Fe_3O_4@PNE@βCD-GOx	204.82	3.20	0.1–30.0	This work

almost twice faster (Fig. S4, see Supplementary Material). The rapid response time demonstrates that the as-prepared catalyst is capable of glucose sensing.

The proposed biosensor was tested using amperometry without stirring conditions. Fig. S5A (see Supplementary Material) shows an amperogram obtained at + 0.3 V for increased concentrations of glucose, and Fig. S5B shows the respective calibration curve presenting a linear relationship between glucose concentration and the current at 45 s. For this technique, the linear range was 0.5–28 mM, the limit of detection was 4.11 μM and the sensitivity was calculated as 179.40 μA μM^{-1} cm^{-2}.

The analytical performances of the SPE/Fe_3O_4@PNE@βCD-GOx biosensor are compared to other research including sensitivity, the limit of detection, and linear range (Table 2). Compared to other enzymatic biosensors in the literature, the proposed glucose biosensor showed good analytical properties for glucose detection, such as good linearity and high sensitivity.

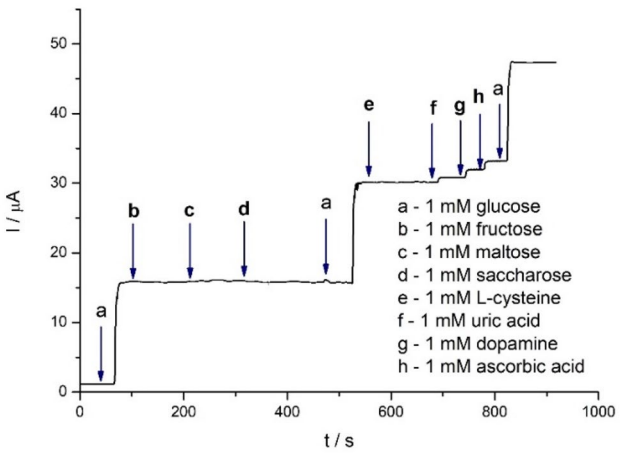

Fig. 6 Interference tests of the biosensor; addition of 1 mM of glucose (a) as the main analyte and 1 mM interferents like fructose (b), maltose (c), saccharose (d), L-cysteine (e), uric acid (f), dopamine (g),
and ascorbic acid (h)

3.5 Interferents tests

The selectivity of the proposed glucose biosensor in the presence of interfering species is one of its most important features. In real samples, some electroactive and non-electroactive species co-exist with glucose and function as interfering molecules. Electroactive species such as ascorbic acid and uric acid are oxidized at the electrode surface and can affect the current responses of hydrogen peroxide produced by the enzymatic reaction. Moreover, nonelectroactive species such as fructose, saccharose, and urea can occur and foul the electrode surface, and affect the final sensor response [37].

To check the influence of interferents on the presented SPE/Fe_3O_4@PNE@βCD-GOx biosensor, an amperometric test was carried out at a potential of 0.3 V and the obtained results were presented in Fig. 6.

The sensor response was measured in the presence of 1 mM glucose and 1 mM interferents like fructose, maltose, saccharose, L-cysteine, uric acid, dopamine, and ascorbic acid. The presence of interferents did not significantly affect the biosensor response (Fig. 6).

3.6 Optimization of the SPE/Fe_3O_4@PNE@βCD-GOx electrode

The SPE/Fe_3O_4@PNE@βCD-GOx biosensor was tested under various temperatures, pH, and mediator concentrations to find the optimum parameters.

The factor that significantly affects the bioactivity of GOx and ultimately the effectiveness of glucose detection is the

Table 3 Measurements of human blood, human serum, and infusion glucose using SPE/Fe_3O_4@PNE@βCD-GOx biosensor and three commercial glucometers ($n=3$)

Sample	Glucose concentration /mM	SPE/Fe_3O_4@PNE@βCD-GOx		Glucometer 1		Glucometer 2		Glucometer 3	
		Found/mM	Recovery/%	Found/mM	Recovery/%	Found/mM	Recovery/%	Found/mM	Recovery/%
Human blood	3.2	3.1 ± 0.1	96.9	2.8 ± 0.3	87.5	2.4 ± 0.4	75.0	2.6 ± 0.2	81.2
	6.9	6.8 ± 0.2	98.6	6.1 ± 0.2	88.4	6.3 ± 0.3	93.3	6.2 ± 0.2	89.5
	14.1	13.8 ± 0.1	97.9	13.0 ± 0.3	92.2	13.5 ± 0.5	95.7	13.6 ± 0.3	96.4
Human serum	2.7	2.6 ± 0.2	96.2	2.4 ± 0.1	88.9	2.1 ± 0.3	77.8	2.5 ± 0.2	92.6
	4.5	4.3 ± 0.1	95.5	3.6 ± 0.2	80.0	3.3 ± 0.5	73.3	4.1 ± 0.4	91.1
	6.2	6.0 ± 0.2	96.8	5.6 ± 0.1	90.3	5.4 ± 0.3	87.1	5.7 ± 0.2	91.9
	8.4	8.2 ± 0.1	97.6	7.8 ± 0.2	92.8	7.4 ± 0.3	88.1	7.6 ± 0.2	90.4
Infusion fluid	5.5	5.4 ± 0.1	98.2	5.2 ± 0.4	95.2	4.1 ± 0.6	74.5	4.8 ± 0.4	87.3

pH of the solution. The optimal pH for glucose oxidase is usually between 5.5 and 7.5, but this varies depending on the immobilization method and the enzyme environment [37]. To check the optimal pH, tests with 2 mM glucose at various values of pH (ranging from 3 to 10) were carried out (Fig. S6A, see Supplementary Material). The enzyme electrode system showed the highest value of the current at pH 7.4, which was selected for further glucose testing.

Moreover to check the temperature stability tests were carried out in the range from 5 to 60 °C (Fig. S6B). The maximum efficiency of the electrode was demonstrated at 40 °C, which is consistent with literature reports [38]. However, due to the slight difference from the ambient temperature, the greater simplicity of the measurements, and the exclusion of any possible evaporation processes, the remaining measurements were carried out. Furthermore, above 50 °C, the sensor electrode showed a decreased amperometric response which may be caused by the denaturation of the protein molecules [38].

The mediator concentration may significantly influence the linear range of a glucose sensor. Previous works showed a lower linear range and low sensitivity at low mediator concentrations, while too-high concentrations limited the enzyme-substrate kinetics [31]. To check the most effective mediator concentration, various values (ranging from 1 to 20 mM) were tested, which are shown in Fig. S7C. Due to a marginal increase in sensor response above 10 mM. This concentration was applied in subsequent testing.

3.7 Test in real glucose samples

To apply the constructed sensor as a mobile POCT sensor, tests on real solutions like human blood, human serum, and infusion fluids were carried out. The research made it possible to check the operation of the system in the environment of interferents and confirm the selectivity and sensitivity. The obtained results are summarized in Table 3. As part of the tests, 3 samples of human blood with different concentration ranges (3.2, 6.9, 14.1 mM) were tested. The high recovery was calculated at the level of 96.9–98.6% ($n=3$) indicating the detection efficiency and the ability of the biosensor to test biological samples as well as potential clinical usefulness. A similar high recovery, ranging from 95.5 to 97.6% was calculated for studies using human serum containing 4 different glucose levels (corresponding to hypoglycemia to diabetes). Finally, glucose in the infusion fluids was also tested with high efficiency (98.2% recovery). The obtained results indicate the high efficiency of glucose detection in the SPE/Fe_3O_4@PNE@βCD-GOx biosensor. Additionally, they were compared with 3 commercial glucometers. Moreover, it can be concluded that the proposed SPE/Fe_3O_4@PNE@βCD-GOx biosensor is characterized by a higher recovery compared to commercial blood glucose detectors available on the market.

3.8 Time stability and reproducibility of the biosensor

The choice of the material for the immobilization of the enzyme is crucial to make an efficient electrochemical detection. The selection of the appropriate material may have a significant impact on the lower variability of measurements over time [22].

The biosensor stability study was tested for SPE/Fe_3O_4@PNE-GOx and SPE/Fe_3O_4@PNE@βCD-GOx for 11 months (Fig. 7). Between the measurements, the electrodes were stored in a refrigerator at 4 °C.

After prolonged storage, the current for the same added glucose decreases. The SPE/Fe_3O_4@PNE-GOx electrode at 8 months showed 75.1% of its initial response. In contrast, the investigated βCD electrode retains over 75.4%

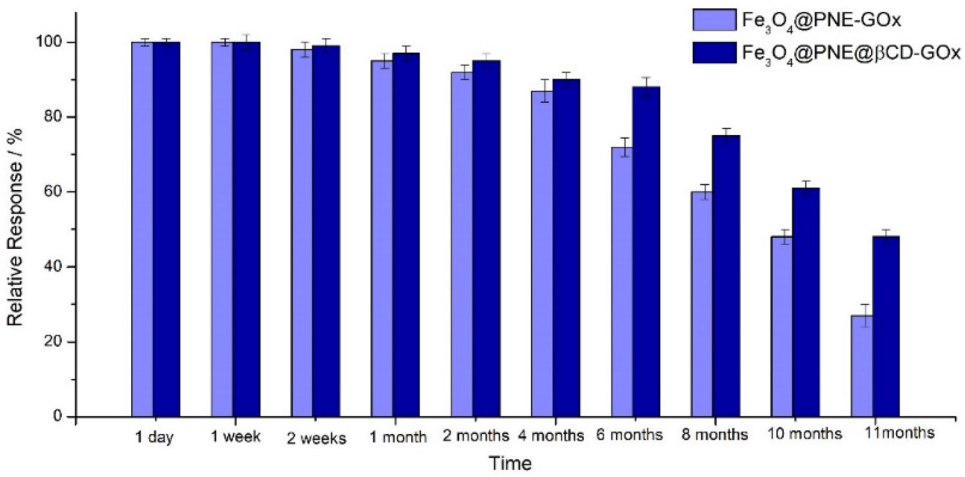

Fig. 7 Comparison of the long-term stability as a relative response to 1 mM glucose for the SPE/Fe_3O_4@PNE-GOx and SPE/Fe_3O_4@PNE@βCD-GOx biosensors ($n = 3$)

Table 4 Comparison of various glucose biosensors against time stability

Biosensor system	Maintained storage stability (%)	Time stability (days)	Reference
Pt/$(CHIT/PAA)_2$/GOx	60.0	60	[39]
GOx- Pt/Pani-Pvs	80.6	40	[40]
ANI-MMT/PtNPs-GOx	91.7	60	[41]
GOx@PAVE-CNTs	92.4	35	[42]
GC/MWCNT/Fe_3O_4/PDA/β-CD-GOx	63.0	210	[22]
SPE/Fe_3O_4@PNE-GOx	75.1	140	[5]
SPE/Fe_3O_4@PNE@βCD-GOx	61.2	330	This work

of its initial performance after 10 months and 61.2% after 11 months. A comparison of the variously constructed biosensors for glucose measurements was presented in Table 4.

Amperometry was used to test the biosensor's repeatability and reproducibility after adding 2 mM of glucose to PBS (10 mM, pH = 7.4). The relative standard deviation (RSD) obtained ($n = 8$) was 3.6%, indicating high repeatability. The reproducibility assay value was 0.6%, indicating that the detection procedure is repeatable.

For the practical uses of electrochemical sensors, good electrochemical repeatability and stability are just as crucial as strong electrocatalytic activity. The stability of the SPE/Fe_3O_4@PNE@βCD-GOx electrode was also assessed by recording the current response in 1 mM glucose solution after 200 consecutive voltammetric cycles (Fig S7A, see Supplementary Material). The proposed biosensor showed a stable character after 200 scans, due to the observed similar response after continuous scans [43].

In addition, the change of biosensor response over time after adding 1 mM glucose was checked (Figure S7B). The biosensor lost 9% of its initial response after 6000 s. This indicates the stable nature of the proposed biosensor. Due to the stable properties of the biosensor, potential application in continuous and real-time measurements is possible.

4 Conclusion

The novel Fe_3O_4@PNE@βCD hybrid nanomaterial was synthesized using straightforward techniques with dispersion-morphological and electrochemical characteristics. An adsorption immobilization of glucose oxidase from *Aspergillus niger* was proposed, which was highly effective.

The addition of β-cyclodextrins, as hypothesized, significantly increased the efficiency and the amount of immobilized enzyme on the support surface (for the Fe_3O_4@PNE, and Fe_3O_4@PNE@βCD nanomaterials with the results 37.8, and 49.1 mg g^{-1}, respectively).

The final nanoplatform was used to build a biosensor based on a screen-printed electrode with a potentiostat compatible with mobile devices. Electrochemical studies indicate that the proposed glucose sensor can be used for glucose measurements in a wide range of glucose concentrations, from hypoglycemia to diabetes. Its most important features are rapid reaction time, high time stability, sensitivity as well as reproducibility, and repeatability. The use of a multicomponent system allowed the extension of the long-live biosensor up to 11 months, enabling selective and sensitive measurements in the same linearity range.

The presented biosensor was also tested on real samples like human blood, human serum, and infusion fluids. The SPE/Fe_3O_4@PNE@βCD-GOx biosensor unveils an attractive alternative as a mobile point-of-care testing tool for glucose measurements. Additionally, it enables real-time measurements outside the laboratory.

Supplementary Information The online version contains supplementary material available at https://doi.org/10.1007/s10800-023-01937-5.

Author contributions AJ: Conceptualization, Investigation, Writing—Original Draft, Writing, Review & Editing. MK: Methodology, Validation, Investigation. TJ: Supervision, Project administration, Funding acquisition, Review & Editing.

Funding This work was financed and prepared as part of a research project supported by the National Science Centre Poland, no. 2017/27/B/ST8/01506. Dr. Artur Jędrzak is also grateful to the Foundation for Polish Science (FNP) for its support through a START scholarship.

Declarations

Conflict of interest The authors declare no competing interests.

References

1. Zhao J, Zheng C, Gao J, Gui J, Deng L, Wang Y, Xu R (2021) Co_3O_4 nanoparticles embedded in laser-induced graphene for a flexible and highly sensitive enzyme-free glucose biosensor. Sens Actuators B 347:130653. https://doi.org/10.1016/j.snb.2021.130653
2. Nichols JH (2011) Blood glucose testing in the hospital: error sources and risk management. J diabetes Sci Technol 5:173–177. https://doi.org/10.1177/193229681100500124
3. Darabdhara G, Bordoloi J, Manna P, Das MR (2019) Biocompatible bimetallic Au-Ni doped graphitic carbon nitride sheets: a novel peroxidase-mimicking artificial enzyme for rapid and highly sensitive colorimetric detection of glucose. Sens Actuators B 285:277–290. https://doi.org/10.1016/j.snb.2019.01.048
4. Bolla AS, Priefer R (2020) Blood glucose monitoring-an overview of current and future non-invasive devices. Diabetes Metab Syndr 14:739–751
5. Jędrzak A, Kuznowicz M, Rębiś T, Jesionowski T (2022) Portable glucose biosensor based on polynorepinephrine@magnetite nanomaterial integrated with a smartphone analyzer for point-of-care application. Bioelectrochemistry 145:108071. https://doi.org/10.1016/j.bioelechem.2022.108071
6. Tang Friesner C, Meyer J, Nippak P (2022) Glucose point-of-care meter operators competency: an assessment checklist. Pract Lab Med 20:e00157. https://doi.org/10.1016/j.plabm.2020.e00157
7. Kuzhandaivel H, Paramasivam K, Manicka S, Nallathambi KS (2023) Nickel-doped CuO/Cu/Cu2O nanocomposite as an efficient electrode for electrochemical non-enzymatic glucose sensor and asymmetric supercapacitor. J Appl Electrochem. https://doi.org/10.1007/s10800-023-01887-y
8. Meskher H, Ragdi T, Thakur AK, Ha S, Khelfaoui I, Sathyamurthy R, Sharshir SW, Pandey AK, Saidur R, Singh P, Sharifian F (2023) A review on CNTs-based electrochemical sensors and biosensors: unique properties and potential applications. Crit Rev Anal Chem 170:1–24. https://doi.org/10.1080/10408347.2023.2171277
9. Meskher H, Hussain CM, Thakur A, Sathyamurthy R, Lynch I, Singh P, Tan KH, Saidur R (2023) Recent trends in carbon nanotube (CNT) based biosensors for fast and sensitive detection of human viruses: a critical review. Nanoscale Adv 5:992–1010. https://doi.org/10.1039/D2NA00236A
10. Munawar T, Sardar S, Nadeem MS, Mukhtar F, Manzoor S, Ashiq MN, Khan SA, Koc M, Iqbal F (2023) Rational design and electrochemical validation of reduced graphene oxide (rGO) supported CeO_2-Nd_2O_3/rGO ternary nanocomposite as an efficient material for supercapacitor electrodes. J Appl Electrochem. https://doi.org/10.1007/s10800-023-01885-0
11. Meskher H, Achi F, Zouaoui A, Ha S, Peacock M, Belkhalfa H (2022) Simultaneous and selective electrochemical determination of catechol and hydroquinone on a nickel oxide (NiO) reduced graphene oxide (rGO) doped multiwalled carbon nanotube (fMWCNT) modified platinum electrode. Anal Lett 55:1466–1481. https://doi.org/10.1080/00032719.2021.2008951
12. Meskher H, Achi F (2022) Electrochemical sensing systems for the analysis of catechol and hydroquinone in the aquatic environments: a critical review. Crit Rev Anal Chem. https://doi.org/10.1080/10408347.2022.2114784
13. Nichols JH (2013) Point-of-care testing. Immunoass Handb. https://doi.org/10.1016/B978-0-08-097037-0.00031-2
14. Khor SM, Choi J, Won P, Ko SH (2022) Challenges and strategies in developing an enzymatic wearable sweat glucose biosensor as a practical point-of-care monitoring tool for type II diabetes. Nanomaterials 12:221. https://doi.org/10.3390/nano12020221
15. Iliescu FS, Ionescu AM, Gogianu L, Simion M, Dediu V, Chifiriuc MC, Pircalabioru GG, Iliescu C (2021) Point-of-care testing-the key in the battle against SARS-CoV-2 pandemic. Micromachines 12:1–33. https://doi.org/10.3390/mi12121464
16. Jońca M, Krótki F, Tomasik P (2021) The effect of disinfecting procedure on the glucose concentration using a personal glucose meter. Prim Care Diabetes 15:848–852. https://doi.org/10.1016/j.pcd.2021.05.010
17. Lee H, Dellatore SM, Miller WM, Messersmith PB (2007) Mussel-inspired surface chemistry for multifunctional coatings. Science 318:426–430. https://doi.org/10.1126/science.1147241
18. Ding YH, Weng LT, Yang M, Yang ZL, Lu X, Huang N, Leng Y (2014) Insights into aggregation/deposition and structure of polydopamine film, Langmuir. ACS J Surf colloids 30:12258–12269. https://doi.org/10.1021/la5026608
19. Lu Z, Teo BM, Tabor RF (2022) Recent developments in polynorepinephrine: an innovative material for bioinspired coatings and colloids. J Mater Chem B 10:7895. https://doi.org/10.1039/D2TB01335E
20. Tan X, Gao P, Li Y, Qi P, Liu J, Shen R, Wang L, Huang N, Xiong K, Tian W, Tu Q (2021) Poly-dopamine, poly-levodopa, and poly-norepinephrine coatings: comparison of physico-chemical and biological properties with focus on the application for blood-contacting devices. Bioact Mater 6:285–296. https://doi.org/10.1016/j.bioactmat.2020.06.024

21. Wu T, Wei X, Ma X, Li J (2017) Amperometric sensing of L-phenylalanine using a gold electrode modified with a metal organic framework, a molecularly imprinted polymer, and β-cyclodextrin-functionalized gold nanoparticles. Microchim Acta 184:2901–2907. https://doi.org/10.1007/s00604-017-2281-5
22. Kuznowicz M, Jędrzak A, Rębiś T, Jesionowski T (2021) Biomimetic magnetite/polydopamine/β-cyclodextrins nanocomposite for long-term glucose measurements. Biochem Eng J 174:108127. https://doi.org/10.1016/j.bej.2021.108127
23. Jędrzak A, Rębiś T, Klapiszewski Ł, Zdarta J, Milczarek G, Jesionowski T (2018) Carbon paste electrode based on functional GOx/silica-lignin system to prepare an amperometric glucose biosensor. Sens Actuators B 256:176–185. https://doi.org/10.1016/j.snb.2017.10.079
24. Abbasi M, Amiri R, Bordbar AK, Ranjbakhsh E, Khosropour AR (2016) Improvement of the stability and activity of immobilized glucose oxidase on modified iron oxide magnetic nanoparticles. Appl Surf Sci 364:752–757. https://doi.org/10.1016/j.apsusc.2015.12.120
25. Torul H, Yarali E, Eksin E, Ganguly A, Benson J, Tamer U, Papakonstantinou P, Erdem A (2021) Paper-based electrochemical biosensors for voltammetric detection of mirna biomarkers using reduced graphene oxide or MoS_2 nanosheets decorated with gold nanoparticle electrodes. Biosensors 11:236. https://doi.org/10.3390/bios11070236
26. Lekshmi IC, Rudra I, Pillai R, Sarika C, Shivakumar MS, Shivakumara C, Konwar SB, Narasimhamurthy B (2020) Enhanced catechol biosensing on metal oxide nanocrystal sensitized graphite nanoelectrodes through preferential molecular adsorption. J Electroanal Chem 867:114190. https://doi.org/10.1016/j.jelechem.2020.114190
27. Phetsang S, Jakmunee J, Mungkornasawakul P, Laocharoensuk R, Ounnunkad K (2019) Sensitive amperometric biosensors for detection of glucose and cholesterol using a platinum/reduced graphene oxide/poly(3-aminobenzoic acid) film-modified screen-printed carbon electrode. Bioelectrochemistry 127:125–135. https://doi.org/10.1016/j.bioelechem.2019.01.008
28. Cao L, Han GC, Xiao H, Chen Z, Fang C (2020) A novel 3D paper-based microfluidic electrochemical glucose biosensor based on rGO-TEPA/PB sensitive film. Anal Chim Acta 1096:34–43. https://doi.org/10.1016/j.aca.2019.10.049
29. World Health Organization. Mean fasting blood glucose. [cited July 18, 2022]. Available from: http://www.who.int/data/gho/indicator-metadata-registry/imr-details/2380.
30. Vukojević V, Djurdjić S, Ognjanović M, Fabián M, Samphao A, Kalcher K, Stanković DM (2018) Enzymatic glucose biosensor based on manganese dioxide nanoparticles decorated on graphene nanoribbons. J Electroanal Chem 823:610–616. https://doi.org/10.1016/j.jelechem.2018.07.013
31. Estrada-Osorio D, Escalona-Villalpando RA, Gutiérrez A, Arriaga LG, Ledesma-García J (2022) Poly-L-lysine-modified with ferrocene to obtain a redox polymer for mediated glucose biosensor application. Bioelectrochemistry 146:108147. https://doi.org/10.1016/j.bioelechem.2022.108147
32. Xia J, Zou B, Liu F, Wang P, Yan Y (2022) Sensitive glucose biosensor based on cyclodextrin modified carbon nanotubes for detecting glucose in honey. J Food Compos Anal 105:104221. https://doi.org/10.1016/j.jfca.2021.104221
33. Faruk Hossain M, Slaughter G (2021) Flexible electrochemical uric acid and glucose biosensor. Bioelectrochemistry 141:107870. https://doi.org/10.1016/j.bioelechem.2021.107870
34. Lin MH, Gupta S, Chang C, Lee CY, Tai NH (2022) Carbon nanotubes/polyethylenimine/glucose oxidase as a non-invasive electrochemical biosensor performs high sensitivity for detecting glucose in saliva. Microchem J 180:107547. https://doi.org/10.1016/j.microc.2022.107547
35. Ge L, Hou R, Cao Y, Tu J, Wu Q (2020) Photoelectrochemical enzymatic sensor for glucose based on Au@C/TiO_2 nanorod arrays. RSC Adv 10:44225–44231. https://doi.org/10.1039/d0ra08920f
36. Zhang BL, Yang Y, Zhao ZQ, Guo XD (2020) A gold nanoparticles deposited polymer microneedle enzymatic biosensor for glucose sensing. Electrochim Acta 358:136917. https://doi.org/10.1016/j.electacta.2020.136917
37. Demirkiran N, Ekinci E, Asiltürk M (2012) Immobilization of glucose oxidase in silica sol-gel film for application to biosensor and amperometric determination of glucose. J Chil Chem Soc 57:1136–1139
38. Chey CO, Ibupoto ZH, Khun K, Nur O, Willander M (2012) Indirect determination of mercury ion by inhibition of a glucose biosensor based on ZnO nanorods. Sensors 12:15063–15077. https://doi.org/10.3390/s121115063
39. Yang M, Yang Y, Liu B, Shen G, Yu R (2004) Amperometric glucose biosensor based on chitosan with improved selectivity and stability. Sens Actuators B 101:269–276. https://doi.org/10.1016/j.snb.2004.01.003
40. Arslan F, Ustabaş S, Arslan H (2011) An amperometric biosensor for glucose determination prepared from glucose oxidase immobilized in polyaniline-polyvinylsulfonate film. Sensors 11:8152–8163. https://doi.org/10.3390/s110808152
41. Zheng H, Liu M, Yan Z, Chen J (2020) Highly selective and stable glucose biosensor based on incorporation of platinum nanoparticles into polyaniline-montmorillonite hybrid composites. Microchem J 152:104266. https://doi.org/10.1016/j.microc.2019.104266
42. Xu S, Zhang Y, Zhu Y, Wu J, Li K, Lin G, Li X, Liu R, Liu X, Wong CP (2019) Facile one-step fabrication of glucose oxidase loaded polymeric nanoparticles decorating MWCNTs for constructing glucose biosensing platform: structure matters. Biosens Bioelectron 135:153–159. https://doi.org/10.1016/j.bios.2019.04.017
43. Mathew M, Sandhyarani N (2013) A highly sensitive electrochemical glucose sensor structuring with nickel hydroxide and enzyme glucose oxidase. Electrochim Acta 108:274–280. https://doi.org/10.1016/j.electacta.2013.07.010

Authors and Affiliations

Artur Jędrzak[1] · Maria Kuznowicz[1] · Teofil Jesionowski[1]

✉ Artur Jędrzak
artur.jedrzak@put.poznan.pl

[1] Institute of Chemical Technology and Engineering, Faculty of Chemical Technology, Poznan University of Technology, Berdychowo 4, Poznan PL-60965, Poland